Molecular Requirements for Targeting the Polyamine Transport System. Synthesis and Biological Evaluation of Polyamine−Anthracene Conjugates

Chaojie Wang,[†,‡] Jean-Guy Delcros,[§] John Biggerstaff,[†] and Otto Phanstiel, IV*,[†]

Groupe de Recherche en Therapeutique Anticancéreuse, Faculté de Médecine, 2, Avenue du Professeur Léon Bernard, 35043 Rennes, France, and Department of Chemistry, P.O. Box 162366, University of Central Florida, Orlando, Florida 32816-2366

Received January 2, 2003

A series of nine N^1-(9-anthracenylmethyl)tetraamines (e.g., Ant-4,4,4-tetraamine) were synthesized and evaluated for cytotoxicity in L1210, α-difluoromethylornithine (DFMO)-treated L1210, Chinese hamster ovary (CHO), and CHO-MG cell lines. Surprisingly, the 3,3,4- and 3,4,3-tetraamine motifs had the same or decreased cytotoxicity in DFMO-treated L1210 cells, whereas the rest of the tetraamine systems were usually more cytotoxic and gave lower IC_{50} values in this treated cell line. The most sensitive derivatives to DFMO treatment were the Ant-4,4,3- and Ant-4,4,4-tetraamine analogues, which were 7 and 5 times more cytotoxic in DFMO-treated L1210 cells, respectively. K_i values for each of the anthracenylmethyl(Ant)-polyamine conjugates were determined in L1210 cells and revealed that these systems are high-affinity ligands for the polyamine transporter (PAT). Mixed results were observed in the CHO and CHO-MG assays. The 4,4,4- and 5,4,4-tetraamine motifs were 3 times more toxic to CHO cells with active polyamine transporters. For example, the Ant-4,4,4-tetraamine conjugate displayed IC_{50} values of 11 μM in CHO cells and 33 μM in CHO-MG cells, a PAT-deficient cell line. This suggested that these derivatives used the PAT in part to access cells. However, most of the other tetraamine derivatives had similar potencies in both the CHO and CHO-MG cell lines. In terms of vector design, higher affinity for the PAT (lower K_i values) did not translate into higher potency for the tetraamine conjugate. In contrast, the related triamine systems, which had micromolar K_i values in L1210 cells, were more efficacious and selective. In one case, the 4,4-triamine motif imparted 150-fold higher potency in CHO cells than the CHO-MG mutant. A deconvolution microscopy study in A375 melanoma cells revealed a rapid internalization of the Ant-4,4,4-triamine as fluorescent vesicles, whereas the Ant-4,4,4-tetraamine remained mostly at the cell surface. These findings help define the key characteristics required for selective delivery of polyamine−drug conjugates into cell types with active polyamine transporters.

Introduction

Vectored or targeted drugs, which have enhanced affinity for cancer cells, would be an important advance in cancer chemotherapy. The polyamine transport system offers one method of targeting specific cell types via the molecular recognition events involved during the importation of exogenous polyamines.[1−13] Prior work in our laboratories evaluated the cytotoxicity and polyamine transporter (PAT) affinity of conjugates containing branched polyamine[1,2] and linear triamine motifs attached to either an anthracene or acridine nucleus.[12,13] Indeed, the preceding article identified certain linear triamines as excellent vectors.[13] In particular, the 4,4-triamine system **1** (Figure 1; **1**, where R = H and both *m* and *n* are 2) had 150-fold higher cytotoxicity in Chinese hamster ovary (CHO) cells (which contained an active polyamine transport system) than in a mutant CHO-MG cell line, which was PAT-deficient.[14,15] We wondered whether this exquisite selectivity for cell types with active polyamine transporters could be further augmented by polyamine chain extension. This report investigated the related N^1-substituted tetraamine systems (e.g., **1**, where R = $-(CH_2)_oNH_2$) and identified important biophysical parameters required to use conjugates between toxic agents (anthracene) and the native polyamines (e.g., putrescine, spermidine, and spermine; **2**−**4** in Figure 1) as vector systems.

While the terminally bis-alkylated polyamines have yielded diverse biological activity ranging from anticancer to antidiarrheal agents,[5,11] their monosubstituted analogues have limited publications describing their use in vector design.[1,2,5,12,13,16−23] This, in part, may stem from their less direct syntheses, which involve several steps.[5,24,25] The conjugates in this report comprise an anthracene nucleus covalently bound to a tetraamine framework. In this manner, cells will be challenged to import the same lethal cargo (anthracene) using various polyamine motifs to assist in cellular entry.[1,2,13]

The anthracene component was selected because of significant preliminary data, which revealed its increased cytotoxicity (lower IC_{50} value) over an acridine analogue in murine leukemia (L1210) cells.[1,2,12,13] The IC_{50} value is the concentration of the drug required to kill 50% of the cell population. Moreover, the anthracene provides a convenient UV "probe" for compound identification and elicits a toxic response from cells upon

* To whom correspondence should be addressed. E-mail: ophansti@mail.ucf.edu. Phone: (407) 823-5410. Fax: (407) 823-2252.
† University of Central Florida.
‡ C.W. is a visiting scholar from the Department of Chemistry, Henan University, Kaifeng, 475001, P. R. China.
§ Groupe de Recherche en Therapeutique Anticancéreuse, Faculté de Médecine.

10.1021/jm020598g CCC: $25.00
Published on Web 05/20/2003

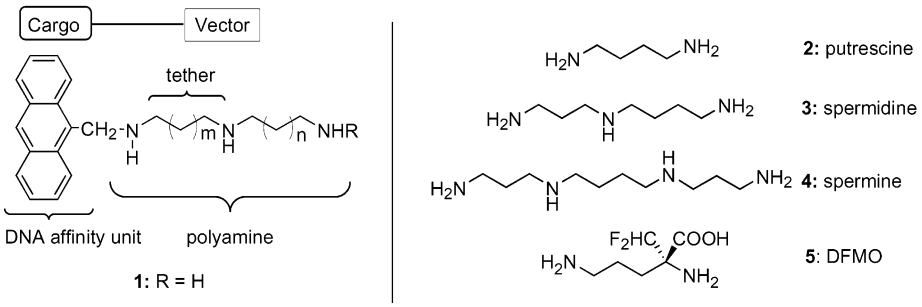

Figure 1. Sample conjugate system, **1**, the native polyamines (**2**−**4**), and DFMO, **5**.

Scheme 1

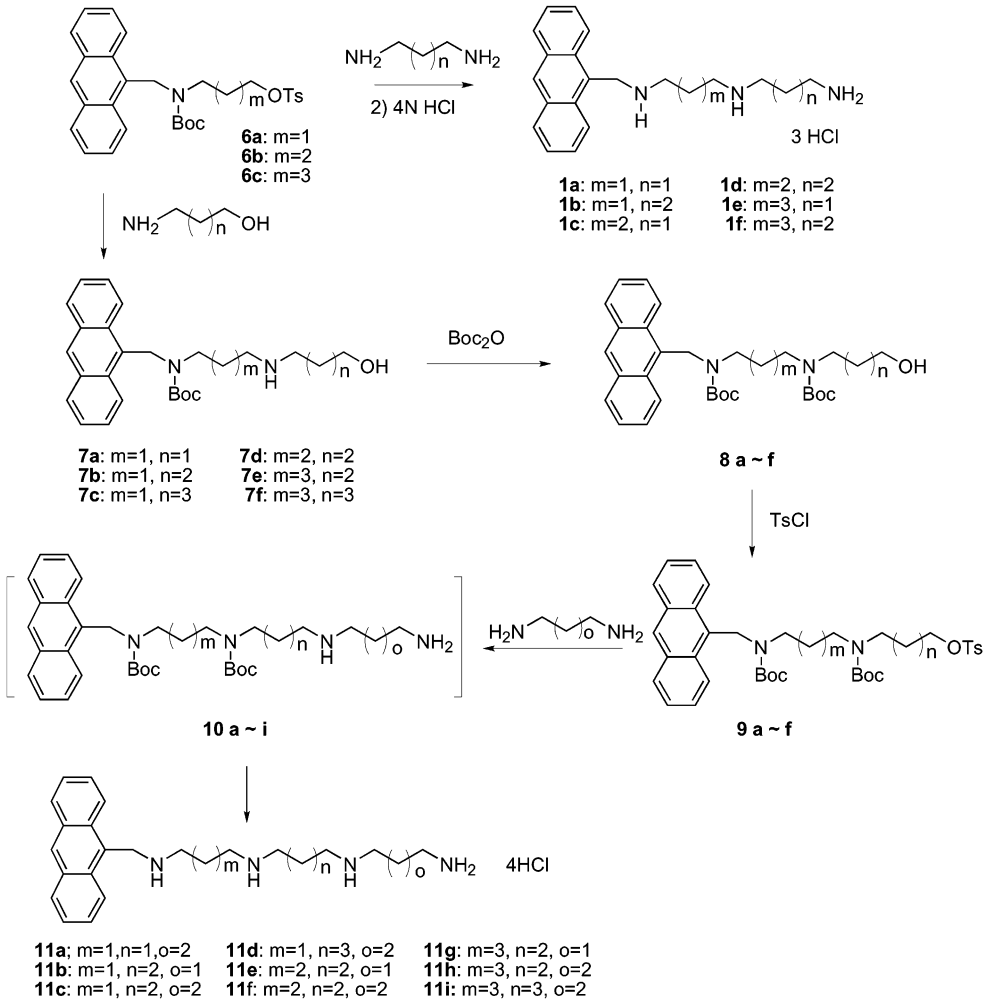

entry (presumably through DNA coordination).[13,26,27] Therefore, a series of tetraamine−anthracene conjugates were synthesized and screened for uptake via the PAT. By judicious choice of amine substrates (e.g., a synthetic library) and proper biological experiments (e.g., IC_{50} and K_i measurements) for selected cell types (murine leukemia L1210, CHO, and CHO-MG cells), one can now comment on transporter affinity and cytotoxicity as a function of polyamine−drug conjugate structure.

Results and Discussion

Synthesis. As shown in Scheme 1, the synthesis of the tetraamine conjugates involved several steps. The modular approach allowed for the introduction of varying chain lengths between the nitrogen centers. Prior work involved the use of amino alcohols as precursors to polyamines.[13,28] Sequential reactions of O-tosylation, tosylate displacement by an amino alcohol (or a diamine), and *tert*-butyloxycarbonylation (Boc introduction) allowed for the rapid construction of the desired scaffolds.[13]

The tosylates **6** were best generated and used as soon as possible.[13] The tosylated compounds **6a**−**c** were reacted with excess amino alcohols to form several derivatives, **7a**−**f**, which were purified and characterized. The triamines **1a**−**f** were synthesized from **6** as described in the preceding article.[13] The target compounds **11a**−**i** were prepared by an analogous route as shown in Scheme 1.

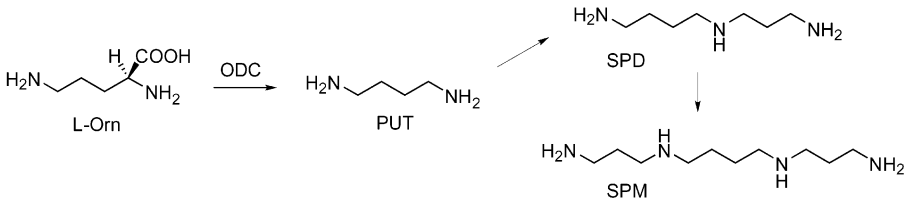

Figure 2. Polyamine biosynthetic pathway.

The tandem Boc introduction and tosylation sequence followed by diamine monoalkylation afforded **10** in good yields. All the *N*-Boc protected compounds **8** (except **8c**) were isolated and characterized. To streamline this multistep sequence, the crude product mixtures were used in the reaction scheme. For example, the crude product of **8c** was used directly in the synthesis of **9c**. The impurities present in **8c** did not affect the subsequest tosylation step. Therefore, one could avoid the tedious column purification of **8**. In fact, it was not necessary to isolate the tosylates **9** either. Nevertheless, two (**9b**, **9d**) of the six compounds of type **9** were isolated to confirm their structure. Using the crude products of **9** for the next substitution step worked well, as expected from our prior success with the alkylation of amino alcohols.[13] The partial *N*-Boc protected tetraamines **10** were prepared in satisfactory yields. They were consumed immediately after purification to get the nine target tetraamines **11** as their HCl salts, which were purified conveniently by washing the solids with absolute ethanol.

An efficient method for the multistep synthesis of the N-monosubstituted tetraamines was developed. The Boc protection and tosylation steps each proceeded in high yield, and the crude products of these compounds could be used directly in the next step. This avoided the lower yields due to isolation steps (with **8** and **9**) and provided for a more efficient synthesis. The total yields of the three steps from intermediates **7** to **10** were generally between 65% and 85% and avoided column chromatography. In short, the tetraamines **11a**−**i** were generated in approximately 30% overall yield from the starting aldehyde.

Biological Evaluation. Three cell lines were chosen for bioassay. L1210 (mouse leukemia) cells were selected to enable comparisons with the published IC_{50} and K_i values known for a variety of polyamine substrates.[5,29] CHO cells were chosen along with a mutant cell line (CHO-MG) in order to comment on selective transport via the PAT.[12]

α-Difluoromethylornithine (DFMO, **5** in Figure 1) is a known ornithine decarboxylase (ODC) inhibitor.[30] ODC is the enzyme responsible for the biosynthesis of putrescine from L-ornithine (see Figure 2). Putrescine (PUT, **2**) is then converted to the longer polyamines, spermidine (SPD, **3**) and spermine (SPM, **4**), via successive aminopropylation steps (Figure 2). Inhibition of ODC blocks intracellular putrescine biosynthesis and leads to a significant increase in polyamine uptake, which allows the cell to acquire polyamines from exogenous sources. Therefore, cells, which are treated with DFMO, should be more susceptible to the polyamine-vectored conjugates and should provide lower IC_{50} values.[11−13] IC_{50} values in L1210 cells with and without DFMO treatment were determined. Conjugates that selectively target the PAT should be more potent with DFMO-treated cells and should provide L1210/(L1210 + DFMO) IC_{50} ratios greater than 1.

Table 1. Comparison of Unsubstituted Polyamine K_i Values of L1210 Cells

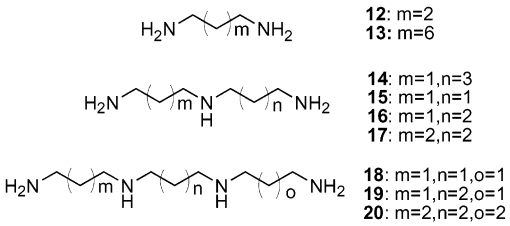

compd (tether)	K_i values (nM) of L1210 cells
1,4-diaminobutane **12** (putrescine)	208200 ± 16340
1,8-diaminoctane **13**	24090 ± 780
(3,5) triamine **14**	8030 ± 500
(3,3) triamine **15**	5120 ± 210
(3,4) triamine **16** (spermidine)	2460 ± 507[a]
(4,4) triamine **17**	2300 ± 80
(3,3,3) tetraamine **18**	1510 ± 120
(3,4,3) tetraamine **19** (spermine)	1340 ± 310
(4,4,4) tetraamine **20**	730 ± 60

[a] K_m value.

The K_i value is a measure of the affinity of the polyamine conjugate for the polyamine transporter and is determined in a competitive assay with radiolabeled spermidine. It should be noted that there are numerous modes of entry for polyamines into cells and that each mode may have a different structure−activity relationship with our synthetic ligands. At present, we were unable to discreetly measure each of these modes of import. Therefore, our K_i measurements reveal the overall transporter affinity of each synthetic conjugate when all these import modes are active in L1210 cells. These collective polyamine import modes will be referred to as the "polyamine transporter" or PAT.

As shown in Table 1, the innate affinities of unsubstituted polyamine systems (**12**−**20**) for the PAT (K_i values) were measured. The following trend toward increasing transporter affinity (lower K_i value) was observed: diamines < triamines < tetraamines. In addition, the tether (number of CH_2 spacer units) between the nitrogen centers had a dramatic effect on the K_i value (e.g., **12** vs **13**). A clear preference for the aminobutyl spacer was evident (e.g., **15** vs **17** and **18** vs **20**). With this preliminary information, we expected a range of activity for the synthetic conjugates **1** and **11**. Indeed, diverse biochemical parameters were obtained with the fluorescent PAT probes listed in Table 2.

The IC_{50} values listed in Table 2 revealed that L1210 cells were more susceptible to triamine conjugates **1a**−**f** than the corresponding tetraamines **11**. This was surprising because the K_i values for the tetraamines (nanomolar range) were significantly lower than the

Table 2. Biological Evaluation of Triamines **1a**−f[13], Tetraamines **11a**−**i**, Other Published Analogues **21**−**25**,[31,12] and Control **28**[13] in L1210 Cells[a]

compd (tether)	L1210 IC_{50} (μM)	L1210 + DFMO IC_{50} (μM)	L1210/(L1210 + DFMO) IC_{50} ratio	L1210 K_i (nM)
1a (3,3)	1.8 ± 0.4	1.4 ± 0.3	1.3	33350 ± 2630
1b (3,4)	0.7 ± 0.3	0.3 ± 0.1	2.3	2500 ± 260
1c (4,3)	0.4 ± 0.1	0.2 ± 0.02	2	6230 ± 580
1d (4,4)	0.3 ± 0.04	0.15 ± 0.1	2	1750 ± 140
1e (5,3)	1.3 ± 0.1	0.7 ± 0.1	1.9	5020 ± 580
1f (5,4)	0.4 ± 0.1	0.3 ± 0.1	1.3	1650 ± 230
11a (3,3,4)	21.8 ± 3.2	21.9 ± 4.3	1.0	108 ± 13
11b (3,4,3)	19.5 ± 2.8	31.9 ± 1.9	0.6	202 ± 8
11c (3,4,4)	10.2 ± 1.6	5.1 ± 0.6	2.0	80 ± 9
11d (3,5,4)	10.7 ± 2.4	7.2 ± 0.1	1.5	90 ± 6
11e (4,4,3)	4.3 ± 0.6	0.6 ± 0.2	7.2	74 ± 5
11f (4,4,4)	7.5 ± 0.3	1.6 ± 0.3	4.7	51 ± 6
11g (5,4,3)	6.4 ± 1.0	2.1 ± 0.7	3.1	99 ± 8
11h (5,4,4)	7.2 ± 0.6	3.8 ± 0.1	1.9	65 ± 5
11i (5,5,4)	7.1 ± 1.2	4.3 ± 0.9	1.6	64 ± 5
21 *N*-ethyl (3,3,3)	>100	ND	ND	7700
22 *N*-ethyl (3,4,3)	99	ND	ND	1700
23 *N*-ethyl (4,4,4)	14	ND	ND	1100
24 (3,4,3) amidoacridiny	18	2.2	8.1	83
25 (3,4,3) aminoacridinyl	2.3	0.6	3.8	83
28 (*N*-butyl) control	14.6 ± 0.1	21.9 ± 3.6	0.7	62300 ± 4200

[a] IC_{50} values were determined after 48 h of incubation with the conjugate. The K_i value of SPM is 1.34 μM, and the K_m value of SPD is 2.46 μM.[12] ND = not determined.

values for the triamine systems (micromolar range). The lower K_i values in Table 2 reflect the higher affinity of the polyamine derivative for the polyamine transporter on the cell surface. The trend clearly indicated a much higher affinity of the tetraamines for the PAT. A priori, one may have anticipated a direct correlation between low K_i values and low IC_{50} values (i.e., high affinity PAT ligands should give more potent drugs). Ironically, the opposite trend was observed!

The presence of DFMO resulted in increased potency (lower IC_{50} values in Table 2) for all conjugates **1** and **11** except **11a** and **11b**. Dramatic increases in potency were observed for specific tetraamines, **11e**−**g**. The most sensitive substrates **11e** and **11f** were 7 and 5 times more cytotoxic in the presence of DFMO, respectively. The results with the other tetraamine systems **11a**−**d** and **11g**−**i** were mixed. With the exception of **1a** and **1f**, the related triamine systems were usually twice as potent in L1210 cells with DFMO treatment.[13] These results suggest that both triamine and tetraamine analogues (**1** and **11**) can use the PAT to access cells.

Why are the tetraamine analogues not more potent? An elementary answer to this dilemma is that the anthracene−triamine architecture is simply more toxic to the cell than the related anthracene−tetraamine construct. This interpretation would assume that the polyamine architecture itself is toxic to the cell and that different polyamine scaffolds will have different cytotoxicities. However, a more intriguing answer may lie in how efficiently these materials (e.g., **1** or **11**) recognize the PAT cell surface receptor and are transferred into the cell (or to their cellular target). In light of the differential PAT affinities (K_i values) observed with the unsubstituted polyamines in Table 1, the latter premise seems to be the most reasonable. In other words, the polyamine "message" is paramount to PAT recognition. Several scenarios may be considered. Even though the N-substituted tetraamines (e.g., **11**) have high affinity for the PAT, inefficient import (very low V_{max}) could explain their reduced cytoxicity. Alternatively, N-substituted tetraamines may inhibit their own transport (as has been reported for other tetraamine derivatives).[12]

An assessment of the conjugates' ability to target the PAT was conducted in two CHO cell lines. The CHO-MG cell line is polyamine-transport-deficient and was isolated for growth resistance to methylglyoxalbis(guanylhydrazone) using a single-step selection after mutagenesis with ethylmethane sulfonate.[14] For the purposes of this study, the CHO-MG cell line represented cells with limited polyamine transporter activity and provides a measure of delivery independent of the PAT. In contrast, the parent CHO cell line represents cell types with active polyamine transport.[14,15] Comparison of conjugate potency in these two lines provided an important screen to detect conjugate delivery via the PAT. For example, a conjugate with high utilization of the transporter would be very toxic to CHO cells but less so to CHO-MG cells.[12,14] Therefore, IC_{50} determinations in these two CHO lines provided a relative ranking of delivery via the PAT. In short, highly selective, vectored conjugates should give high CHO-MG/CHO IC_{50} ratios.

As shown in Table 3, the triamines were usually more potent than the tetraamines in CHO cells. Biological evaluation of triamines **1a**−**f** and tetraamines **11a**−**i** in the two CHO cell lines also revealed striking preferences by certain polyamine architectures for the PAT. As mentioned previously, the 4,4-triamine **1d** displayed nearly 150-fold higher cytotoxicity in the CHO over the CHO-MG cell line.[13] In contrast, the most selective tetraamines **11f** and **11h** were only 3-fold more potent in the CHO cell line. These findings demonstrate that CHO and CHO-MG IC_{50} comparisons are an excellent way to rank polyamine vectors and their transport.[12] The cytotoxicity of the triamines **1** in the CHO lines correlated nicely with the L1210 IC_{50} and K_i results.[13] Therefore, the triamine systems seem to be well-behaved systems that give consistent data in all three cell lines.

Table 3. Biological Evaluation of Triamines **1a**−**f**,[13] Tetraamines **11a**−**i**, Other Published Conjugates **24** and **25**,[12] and Control **28**[13] in CHO-MG and CHO Cell Lines

compd (tether)	CHO-MG IC_{50} (μM)	CHO IC_{50} (μM)	CHO-MG/CHO IC_{50} ratio
1a (3,3)	3.4 ± 0.5	1.9 ± 0.4	1.8
1b (3,4)	8.8 ± 1.2	2.5 ± 0.7	3.5
1c (4,3)	9.5 ± 1.1	0.4 ± 0.1	24
1d (4,4)	66.7 ± 4.1	0.45 ± 0.1	148
1e (5,3)	10.1 ± 1.2	4.1 ± 0.5	2.5
1f (5,4)	57.3 ± 2.9	1.5 ± 0.1	38
11a (3,3,4)	41.5 ± 3.5	44 ± 0.0	0.9
11b (3,4,3)	75.7 ± 7.4	59.7 ± 6.5	1.3
11c (3,4,4)	52.8 ± 2.6	31.1 ± 7.3	1.7
11d (3,5,4)	41.7 ± 0.2	34.9 ± 1.3	1.2
11e (4,4,3)	2.8 ± 0.4	4.0 ± 1.4	0.7
11f (4,4,4)	33.2 ± 1.7	10.6 ± 0.0	3.1
11g (5,4,3)	33.5 ± 3.5	18.1 ± 3.5	1.9
11h (5,4,4)	30.8 ± 0.4	9.9 ± 1.6	3.1
11i (5,5,4)	5.7 ± 1.6	4.0 ± 0.8	1.4
24 (3,4,3) amidoacridinyl	21	17	1.2
25 (3,4,3) aminoacridinyl	7.2	2.3	3.1
28 (*N*-butyl) control	11.2 ± 2.3	10.5 ± 2.0	1.1

In contrast, the tetraamines were more complex and few guiding trends were evident. For example, the 4,4,4 tetraamine **11f** had the highest affinity for the PAT as evidenced by its low K_i value (51 nM) in L1210 cells, but this feature only correlated with a 3-fold increase in cytotoxicity with CHO cells over their CHO-MG counterparts. In short, the high PAT affinity of these tetraamine ligands did not translate to dramatic increases in cytotoxicity in either the L1210 or CHO cell lines.

In terms of vector design, the 4,4-triamine motif (homospermidine) was found to be the optimal chemical signal to gain entry to cells via the PAT. For example, conjugates **1d, 11c**, **11f**, and **11h** each present the terminal 4,4-triamine "signal" to the PAT receptor and each gave the highest selectivity, i.e., the highest (CHO-MG/CHO) IC_{50} ratio, in their respective classes. Of these four, the triamine **1d** clearly gave the best selectivity profile. Furthermore, **1d** had relatively low toxicity in cells with low PAT activity and high toxicity in cells with high polyamine transport activity.

Other authors have shown differences in transporter affinity (K_i) and L1210 cytotoxicity (IC_{50}) behavior for related *N*-monoalkyltetraamine architectures.[31] As shown in Table 2, the terminal monoethylated tetraamines **21**, **22**, **23** were found by Bergeron et al. to have K_i values in the micromolar range (7.7, 1.7, and 1.1 μM, respectively) and higher 48 h IC_{50} values (≥14 μM). The *N*-ethyl substrates **22** and **23** allow for direct comparison to our findings with the *N*-anthracenylmethyl 3,4,3-tetraamine **11b** and the 4,4,4-tetraamine **11f**. A priori one may have expected that polyamines with bulky N substituents would be poor ligands for the polyamine transporter. However, the comparison suggests that the bulky anthracenylmethyl substituent actually enhances the PAT binding affinity and cytotoxicity of the polyamine conjugate in vitro. As shown in Table 2, the tetraamines **11**, **24**, and **25** have nanomolar K_i values in L1210 cells. Delcros and co-workers have shown a similar effect with N^1-acridinyl substituted tetraamines.[12] Therefore, N^1-substitution with an appended aromatic ring system like the anthracenylmethyl or acridinyl unit leads to a large decrease in the K_i value (see Table 2 for K_i values for **22** vs **11b**, **24**, and **25**). In short, aromatic substituents seem to impart higher affinity for cell-surface receptors.

Comparison of **11b** (Ant-3,4,3) with **24** and **25** suggests that the distally tethered acridine motifs present in **24** and **25** impart higher potency than the anthracenylmethyl substituent when tested in CHO cells (Table 3). Interestingly, DFMO treatment of L1210 cells resulted in the expected increase in potency of **24** and **25** but surprisingly gave decreased cytotoxicity for **11b** (Table 2). This seems to be an anomaly and unique for the 3,4,3-tetraamine motif in **11b**, since it was the only entry in Table 2 with an IC_{50} ratio of <1. Ironically, this 3,4,3 motif is equivalent to N^1-substituted spermine (SPM), a native polyamine. The other polyamine homologues all had IC_{50} ratios of ≥1 in Table 2. The differences in cytotoxicity (between **11b**, **24**, and **25**) may stem from the different degrees of conformational freedom imparted by the chain length available to the longer tether of the acridine substitutent as well other modes of cellular entry for the acridine ring system.[1,2,12] A more direct structural comparison of the anthracenylmethyl and acridine nuclei was conducted previously with the branched polyamine motifs **26** and **27**.[1,2] Earlier work demonstrated that the *N*-(9-anthracenemethyl) substituent of **26** was more potent than the corresponding *N*-(9-aminoacridinyl) substituent in **27** (47 h IC_{50} values of 13 μM for **26** and 75 μM for **27**).[1,2] Nevertheless, the fact that **24** and **25** were more cytotoxic than **11b** suggested that further structural modification is accommodated by the PAT as long as the proper "polyamine message" is in place.

It should be noted that the control *N*-butyl derivative **28**[13] (shown in Figure 3) gave no enhancement in cytotoxicity when dosed in the presence of DFMO and had a high K_i value (62 300 nM, Table 2) in L1210 cells. Thus, an *N*-butylanthracene moiety like **28** has little affinity for the PAT and likely enters the cell via another pathway. Moreover, as shown in Table 3, this *N*-butyl control showed virtually no preference in targeting CHO over CHO-MG cells. Collectively, these observations further support the ability of certain cell types to recognize the conjugates via their polyamine motifs.

Are tight binders such as the tetraamines **11** localized at the cell membrane and internalized more slowly? A possible answer is that the tetraamines, in general, rapidly suppress PAT activity and limit their own uptake by the transporter.[12] This premise is supported by the observed low K_i values (both were 83 nM) and low CHO-MG/CHO IC_{50} ratios for **24** (1.2) and **25** (3.1), which are similar to those of the other tetraamines tested (**11**).

To further address this issue, we conducted a qualitative study using deconvolution microscopy to compare the relative rates of delivery of the 4,4-triamine **1d** and the 4,4,4-tetraamine **11f** "probes" into A375 melanoma cells. Melanoma cells were chosen because of their large size and susceptibility to polyamine analogues.[6] A375 cells were incubated with the respective conjugate (at 10 μM) for 3 min. A series of optical "slices" of the resultant cells were obtained, and one slice was chosen to best represent the sample overall. The anthracene component was easily tracked via its diagnostic fluorescence properties and is shown in white and gold in Figure 4. The UV spectra of the anthracene conjugates suggest a consistent λ_{max} near 364 nm and an emission maxima near 417 nm. The relative levels of fluorescence

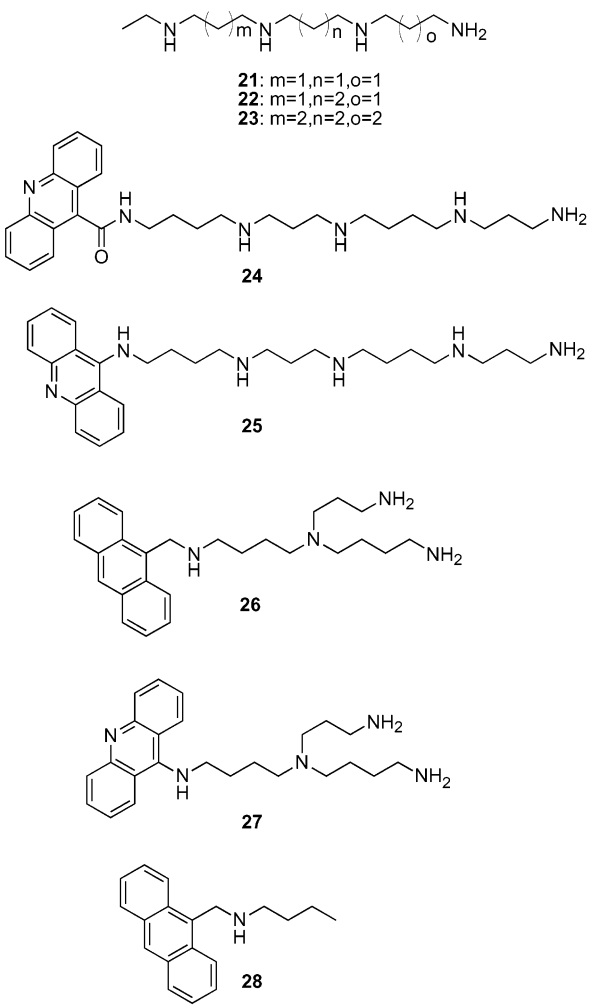

Figure 3. Other polyamine conjugates **21**−**27** and the *N*-butyl control **28**.

suggested different internalization rates and localization behavior between the two probes (**1d** and **11f**). Panels 1 and 3 in Figure 4 are control samples, wherein after incubation with the respective polyamine conjugate, the cells were first fixed with paraformaldehyde and then washed. Copious amounts of triamine **1d** (panel 1) or **11f** (panel 3) remain associated with the cell surface. However, when the cells were first washed with fresh buffer and then fixed with paraformaldehyde, a different result was obtained. As shown in Figure 4, the triamine conjugate **1d** (panel 2) clearly accessed the cell more rapidly than **11f** (panel 4) as evidenced by the greater number of fluorescent vesicles inside the cell**.** The triamine probe **1d** was mainly sequestered as internal vesicles, whereas the tetraamine counterpart **11f** was nearly exclusively bound to the cell surface with few vesicles being formed during this short time period. The limited amount of triamine at the surface is consistent with the lower binding affinity of this probe to PAT (Table 2) and presumably to other membrane receptors. A comparison of panels 1 and 2 (with **1d**) revealed that both the surface-bound and unbound triamines were more efficiently washed away from the cell surface in the workup step.

These findings are significant because they are the first *comparative* observations of polyamine vectors in action. Moreover, they offer a possible explanation of

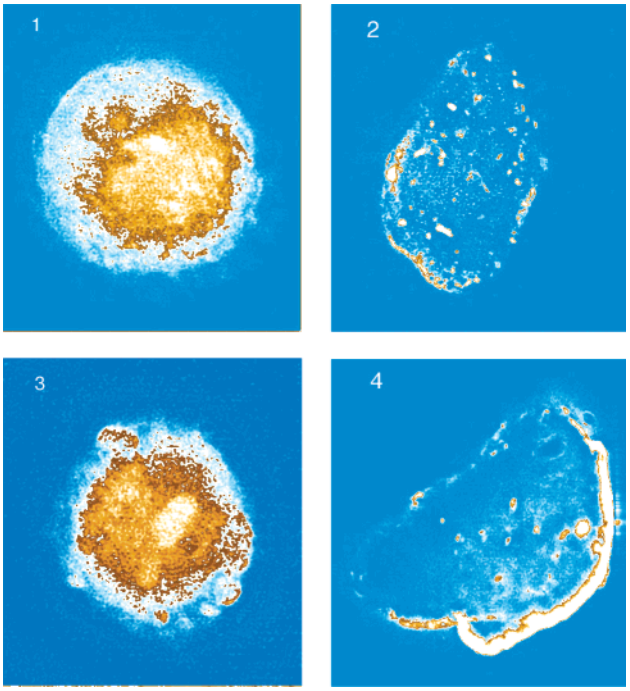

Figure 4. Deconvolution microscopy images of A375 cells treated with **1d** (panels 1and 2) and **11f** (panels 3 and 4). Panels 1 and 3 represent cells incubated with **1d** and **11f**, respectively, at 10 μM for 3 min and then fixed with paraformaldehyde and washed with buffer. Panels 2 and 4 represent cells that were incubated with **1d** and **11f**, respectively, washed with buffer, and then fixed with paraformaldehyde.

why the tetraamines are less potent. The high-affinity tetraamine ligands bind rapidly to the cell surface by interacting with the PAT and other cell-surface receptors. Moreover, they appear to be less internalized than the related triamines. Indeed, slower uptake is likely related to their lower potency. The observation that the high-affinity tetraamine ligands remain bound to the cell surface even after washing is also noteworthy. This finding provides a rationale for earlier observations wherein PAT activity was not restored upon removal of the tetraamine drug from the culture medium.[12] Indeed, this "sticky tetraamine" phenomenon may be a property of N-substituted tetraamines in general.

There is a strong possibility that the tetraamines **11** are associated with other non-PAT receptors on the cell surface. As seen previously in panel 4, the widespread distribution of **11f** remaining across the cell surface (even after washing) suggests that numerous nonlocalized interactions occurred between **11f** (at 10 μM) and the cell membrane. This observation was not surprising because polyamines have a high affinity for membrane constituents (such as phospholipids and glycoproteins)[32] that is strongly dependent on the number of amino groups. Moreover, the large aromatic moiety should favor bridging interactions between both proteins and lipids in the membrane. Earlier work by Delcros and others revealed that L1210 cells were still susceptible to tetraamine−acridine conjugates (like **25**) even in the presence of 500 μM spermidine (SPD). On the basis of the K_i values determined, this quantity of SPD should have completely inhibited the uptake of the conjugate **25**. Indeed, excess SPD in the culture medium only partially reduced the amount of **25** associated with the cells.[12] This finding suggested that 500 μM SPD was

unable to outcompete for the bound N-substituted tetraamine sites and that unsubstituted triamines such as SPD have a lower affinity for these alternative tetraamine docking sites. Moreover, prior work by other authors has shown that spermine (SPM, i.e., the 3,4,3-tetraamine) reduces the lateral mobility of glycoproteins inside the membrane.[33] In addition, Ballas has shown that interactions between an exogenous tetraamine (SPM) and erythrocyte membranes resulted in decreased membrane deformability.[33] Because the N^1-aryl-substituted tetraamines likely have a much higher affinity for the membrane than SPM, they should have a greater influence on the membrane. Strong binding of tetraamines may impair both the membrane structure and its functions. Such an event may ultimately limit tetraamine import.

On the other hand, N^1-substituted triamines such as **1d** are bound less tightly to the cell surface. As shown in Figure 4 (panels 1 and 2), the loosely bound triamines can be washed off the cell surface with aqueous buffer. The triamines likely act as reversible ligands, which are more selective in bonding to their cellular target, the PAT. In an anthropomorphic sense, the triamines present their "polyamine message" or "passport" to various cellular gates of entry. They reversibly search along the cell surface and rapidly enter the correct gate. In contrast, the tetraamines present "valid passports" to numerous surface targets (gates) and are held tightly to the cell surface as they interact with these numerous "gates". These multiple binding events likely disrupt the stability of the membrane and result in slow tetraamine entry into the cell. This speculation is supported somewhat by Figure 4 (panel 4), wherein the tetraamine remains bound to a large portion of the cell surface (even after a buffer wash) and fewer vesicles are apparent inside the cell (compared to panel 2). Another explanation may be that the tetraamine interacts strongly with the PAT gate itself and limits its own import. Regardless of the rationale, the lower PAT affinity of the triamines provided a more selective vector.

The findings are also consistent with a model proposed by Cullis and Poulin.[6,34] First, polyamines bind to a surface receptor, which results in membrane envagination (endocytosis) to create polyamine-rich vesicles inside the cell. The derivative may then be exported out of this vesicle to a particular cellular compartment via a cationic symporter.[6] Indeed, panel 4 in Figure 4 seems to have captured this endocytosis event in action. According to this model, in order to exit the vesicle (via the putative cationic symporter), the conjugate must dissociate from its vesicular PAT receptor. Since the tetraamines are high-affinity PAT ligands, they likely dissociate more slowly from the receptor. In contrast, the triamines have lower binding affinities and should dissociate more rapidly from the internalized PAT receptor to exert their toxic effect. Although further kinetic studies are needed, this rationale would also explain why the triamines are more potent and yet have higher K_i values.

A polyamine transporter gene has not yet been identified in mammalian cells. In fact, little is known about the structural aspects of the polyamine transporter (PAT) itself. However, recent reports by Frannson and co-workers have suggested that proteoglycans play a role in polyamine transport.[32,35,36] Proteoglycans are composed of glycosaminoglycan chains covalently linked to protein, and expression of cell-surface proteoglycans is required for the binding of many extracellular substrates.[32] Indeed, inhibition of polyamine biosynthesis with DFMO resulted in an increase of cell-associated proteoglycans exhibiting higher affinity for spermine in a human lung fibroblast study.[32] The data indicated a specific role for heparan sulfate proteoglycans (HSPG) in the uptake of spermine by fibroblasts. These provocative results suggest that proteoglycan-mediated polyamine transport may play an important role in future drug delivery strategies.[37,38] The current report also provides new fluorescent probes needed to evaluate these interesting new pathways.

In summary, the polyamine transporter is capable of distinguishing between isomeric systems that have the same overall length but a different separation of point charges.[5,31,39−42] The current study has identified some of the optimal motifs and the necessary biophysical parameters in order to initiate transport via this pathway.

Conclusions

An efficient modular synthesis of N^1-substituted polyamines containing different tether lengths between nitrogen centers was developed. This new methodology should contribute to the limited synthetic approaches used to access linear polyamines.[43] All triamine conjugates **1** and most tetraamines (except **11a** and **11b**) had higher potency in DFMO-treated L1210 cells. High PAT affinity (low nanomolar K_i values) did not translate into a more efficacious drug. A survey of different polyamine vectors revealed that the respective 4,4- and 5,4-triamine systems had 150-fold and 38-fold selectivity for CHO cells containing active polyamine transporters. Optimal use of this transporter seems to require a balance involving moderate PAT binding affinity and conjugate internalization. Future studies will use these fluorescent polyamine probes to further delineate the delivery differences. In summary, selective vector motifs were identified that ferry drugs into cancer cell types via the PAT.

Because many cancer cell lines have high PAT activity, especially when dosed with DFMO,[6,44−46] these results suggest a new anticancer strategy predicated upon the use of a triamine vector to shuttle appended drug "cargoes" selectively into cells. Future work will evaluate this strategy in a mouse leukemia model.

Experimental Section

Materials. Silica gel (32−63 μm) and chemical reagents were purchased from commercial sources and used without further purification. All solvents were distilled prior to use. ^{1}H and ^{13}C NMR spectra were recorded at 300 and 75 MHz, respectively. TLC solvent systems are based on volume percent, and NH_4OH refers to concentrated aqueous NH_4OH. All tested compounds provided satisfactory elemental analyses, which were performed by Atlantic Microlabs (Norcross GA). High-resolution mass spectrometry was performed by Dr. David Powell at the University of Florida mass spectrometry facility.

Biological Studies. Murine leukemia cells (L1210), CHO, and CHO-MG cells were grown in RPMI medium (Eurobio, Les Ulis, France) supplemented with 10% fetal calf serum,

2 mM glutamine (2 mM), penicillin (100 U/mL), and streptomycin (50 μg/mL) (BioMerieux, Marcyl'Etoile, France). L-Proline (2 μg/mL) was added to the culture medium for CHO-MG cells. Cells were grown at 37 °C under a humidified 5% CO_2 atmosphere. Aminoguanidine (2 mM) was added to the culture medium to prevent oxidation of the drugs by the enzyme (bovine serum amine oxidase) present in calf serum. Trypan blue staining was used to determine cell viability before the initiation of a cytotoxicity experiment. Typically, samples contain less than 5% trypan blue positive cells (dead). For example, L1210 cells in the early to mid log phase were used.

IC_{50} Determinations. Cell growth was assayed in sterile 96-well microtiter plates (Becton-Dickinson, Oxnard, CA). L1210 cells were seeded at 5×10^4 cells/mL of medium (100 μL/well). Single CHO and CHO-MG cells harvested by trypsinization were plated at 2×10^3 cells/mL. Drug solutions (5 μL per well) of appropriate concentration were added at the time of seeding for L1210 cells and after an overnight incubation for CHO and CHO-MG cells. In some experiments DFMO (5 mM) was added in the culture medium at the time of drug addition. After exposure to the drug for 48 h, cell growth was determined by measuring formazan formation from 3-(4,5-dimethylthiazol-2-yl)-2,5-diphenyltetrazolium using a Titertek Multiskan MCC/340 microplate reader (Labsystems, Cergy-Pontoise, France) for absorbance (540 nm) measurements.[47]

K_i Procedure. The ability of the conjugates to interact with the polyamine transport system were determined by measuring competition by the conjugates against radiolabeled spermidine uptake in L1210 cells. The same procedure was used to obtain the data listed in Tables 1 and 2. Initially, the K_m value of spermidine transport was determined in a reaction volume of 600 μL of Hanks' balanced salt solution (HBSS) containing 3×10^6 cells/mL in the presence of 0.5, 1, 2, 4, 6, and 8 μM [^{14}C]-spermidine. The cell suspensions were incubated at 37 °C for 10 min. The reaction was stopped by adding 3 mL of ice-cold phosphate-buffered saline (PBS). The tubes were centrifuged, and the supernatant was removed. The cell pellets were then washed twice with ice-cold PBS, and the supernatant was removed. The pellet was broken by sonication in 500 μL of 0.1% Triton in distilled water. Two hundred microliters of the cell lysate was transferred into a 5 mL scintillation vial containing 3 mL of Pico-Fluor 15. The respective radioactivity of each sample was measured using a scintillation counter. The K_m value of spermidine transport was determined by the Lineweaver−Burke analysis as described.[48]

The ability of conjugates to compete for [^{14}C]-spermidine uptake was determined in L1210 cells by a 10 min uptake assay in the presence of increasing concentrations of competitor, using 1 μM [^{14}C]-spermidine as substrate. K_i values for inhibition of spermidine uptake were determined using the Cheng−Prusoff equation[49] from the IC_{50} value derived by iterative curve fitting of the sigmoidal equation describing the velocity of spermidine uptake in the presence of the respective competitor.[50,51] Cell lines (murine leukemic L1210 cells) were grown and maintained according to established procedures.[7,52] Cells were washed twice in HBSS prior to the transport assay.

Deconvolution Microscopy. The microscope system included an Applied Precision (Issaquah, WA) Deltavision system equipped with a Nikon Eclipse TE200 inverted microscope. Image deconvolution was performed using Applied Precision SoftWorX software. Detached melanoma A375 cells[13] were incubated for 3 min with **1d** and **11f** (10 μM) at 37 °C in a culture medium (containing 10% fetal bovine serum in RPMI-1640 media containing phenol red and an antibiotic cocktail). The cells were then washed with fresh media and centrifuged, and the supernatant was removed. The cellular pellet was resuspended in fresh media, fixed with paraformaldehyde, placed onto a microscope slide, and imaged by the deconvolution microscope. This technique provides an image of the entire cell by using software to overlay a series of planar images (or slices) to give a stacked translucent view of the entire cell. The lightest regions in Figure 4 contain the highest concentration of the fluorescent conjugate.

Preparation of Triamines 1a−f and 6a−c. The synthesis and full characterization of triamines **1a−f** and **6a−c** were reported in the preceding article.[13]

General Procedure for the *N*-Boc Protection (Preparation of 8). A solution of **7** (5 mmol) in pyridine/methanol (1:5 v/v, 20 mL) was stirred at 0 °C for 10 min. A solution of di-*tert*-butyl dicarbonate (7.5 mmol) in methanol (5 mL) was added dropwise over 10 min. The mixture was stirred for 1 h. The temperature was then allowed to gradually rise to room temperature, and the reaction mixture was stirred overnight. The mixture was evaporated under reduced pressure. The residue was dissolved in methylene chloride and washed with deionized water several times. The organic layer was separated, dried with anhydrous Na_2SO_4, filtered, and concentrated. The residue could be purified by flash column chromatography on silica gel or be used in the next step without further purification.

General Procedure for the Tosylation of the Hydroxy Group (Preparation of 9). The solution of the *N*-Boc protected **8** (5 mmol) in dry pyridine (20 mL) was stirred at 0 °C for 10 min. *p*-Toluenesulfonyl chloride (TsCl, 7.5 mmol) was added in small portions over 30 min. The mixture was stirred for an additional hour, and then the reaction flask was placed in a refrigerator (0−5 °C) overnight. The mixture was poured into 200 mL of ice/water, and a viscous liquid typically precipitated. After the upper water layer was decanted off, the viscous liquid or hemisolid was dissolved in methylene chloride and washed with deionized water several times. The organic layer was separated, dried with anhydrous Na_2SO_4, filtered, and concentrated. The residue could be purified by column chromatography on silica gel or used in the next step without further purification.

General Procedure for the Substitution of the Tosylated Compounds with the Amino Alcohols (Preparation of 7) or Diamines (Preparation of 10). The tosylated compounds **6** (1 mmol) and amino alcohols (5 mmol) (or tosylates **9** with diamines) were dissolved in acetonitrile (10 mL), and the mixture was then stirred at 75 °C under N_2 overnight. After a check for the disappearance of the tosylate by TLC, the solution was concentrated under reduced pressure. The residue was dissolved in CH_2Cl_2 (20 mL) and washed three times with saturated aqueous sodium carbonate. The organic layer was separated, dried with anhydrous sodium sulfate, filtered, and concentrated under vacuum. The residue was purified by flash column chromatography on silica gel. The purified products **7** (or **10**) were used in the next deprotection step immediately.

General Procedure for the Amino Group Deprotection (Preparation of 11). The *N*-Boc protected N^1-(anthracen-9-ylmethyl)tetraamines (**10**, 0.5 mmol) were dissolved in ethanol (5 mL), and the mixture was stirred at 0 °C for 10 min. A 4 N HCl (8 mL) solution was then added dropwise at 0 °C. The reaction mixture was stirred at room temperature overnight. The solution was then concentrated under reduced pressure (water bath maintained below 60 °C), and a bright yellow solid precipitated. The solid was washed several times with absolute ethanol and provided the pure target compound **11**.

Anthracen-9-ylmethyl[3-(3-hydroxy-propylamino)propyl]carbamic acid *tert*-butyl ester (7a): pale-yellow viscous liquid; yield 51%; $R_f = 0.53$, chloroform/methanol/NH_4OH, 90:10:1; ^{1}H NMR δ 8.39 (s, 1H), 8.37 (d, 2H), 7.95 (d, 2H), 7.43 (m, 4H), 5.42 (br s, 2H), 3.60 (t, 2H), 2.82 (br s, 2H), 2.42 (t, 2H), 2.18 (t, 2H), 1.50 (m, 11H), 1.24 (br s, 2H); ^{13}C NMR δ 155.78, 131.53, 131.44, 129.47, 128.44, 126.61, 125.23, 124.26, 80.24, 64.19, 49.66, 47.29, 43.06, 41.46, 30.98 (2C), 28.95 (3C). HRMS (FAB) calcd for $C_{26}H_{35}N_2O_3$ $(M + H)^+$: 423.2648. Found: 423.2657.

Anthracen-9-ylmethyl[3-(4-hydroxybutylamino)propyl]carbamic acid *tert*-butyl ester (7b): pale-yellow viscous liquid; yield 67%; $R_f = 0.38$, chloroform/methanol/NH_4OH, 90:10:1; ^{1}H NMR δ 8.40 (s, 1H), 8.38 (d, 2H), 8.00 (d, 2H), 7.45 (m, 4H), 5.50 (br s, 2H), 3.44 (t, 2H), 3.38 (br s, 2H), 2.84 (br s, 2H), 2.28 (t, 2H), 2.20 (t, 2H), 1.50 (br s, 11H), 1.40 (br s,

2H), 1.30 (br s, 2H); ^{13}C NMR δ 155.67, 131.53, 131.44, 129.47, 128.46, 126.64, 125.25, 124.25, 80.34, 62.68, 49.49, 46.86, 43.02, 41.48, 32.62 (2C), 28.94 (3C, CH_3), 28.65. HRMS (FAB) calcd for $C_{27}H_{37}N_2O_3$ $(M + H)^+$: 437.2804. Found: 437.2800.

Anthracen-9-ylmethyl[3-(5-hydroxypentylamino)propyl]carbamic acid *tert*-butyl ester (7c): pale-yellow viscous liquid; yield 66%; $R_f = 0.38$, chloroform/methanol/NH_4OH, 92:8:1; ^{1}H NMR δ 8.40 (s, 1H), 8.38 (d, 2H), 7.98 (d, 2H), 7.45 (m, 4H), 5.45 (br s, 2H), 3.50 (t, 2H), 2.84 (br s, 2H), 2.25 (t, 2H), 2.20 (t, 2H), 1.50 (br s, 11H), 1.40 (br s, 2H), 1.28 (br s, 4H); ^{13}C NMR δ 155.81, 131.53, 131.44, 129.43, 128.39, 126.54, 125.21, 124.36, 80.09, 62.69, 49.77, 47.55, 43.08, 41.33, 32.79 (2C), 29.84, 28.92 (3C, CH_3), 23.73. HRMS (FAB) calcd for $C_{28}H_{39}N_2O_3$ $(M + H)^+$: 451.2961. Found: 451.2975.

Anthracen-9-ylmethyl[4-(4-hydroxybutylamino)butyl]carbamic acid *tert*-butyl ester (7d): pale-yellow viscous liquid; yield 74%; $R_f = 0.36$, chloroform/methanol/NH_4OH, 92:8:1; ^{1}H NMR δ 8.42 (s, 1H), 8.39 (d, 2H), 8.01 (d, 2H), 7.50 (m, 4H), 5.50 (br s, 2H), 3.50 (t, 2H), 2.80 (br s, 2H), 2.40 (t, 2H), 2.20 (t, 2H), 1.58 (br s, 13H), 1.24 (m, 2H), 1.10 (m, 4H); ^{13}C NMR δ 155.77, 131.54, 131.49, 129.43, 128.35, 126.56, 125.24, 124.37, 80.12, 62.84, 49.66, 48.99, 44.70, 41.46, 32.98, 29.18, 28.95 (3C, CH_3), 26.99, 26.46. HRMS (FAB) calcd for $C_{28}H_{39}N_2O_3$ $(M + H)^+$: 451.2961. Found: 451.2947.

Anthracen-9-ylmethyl[5-(4-hydroxybutylamino)pentyl]carbamic acid *tert*-butyl ester (7e): pale-yellow viscous liquid; yield 90%; $R_f = 0.66$, chloroform/methanol/NH_4OH, 92:8:2; ^{1}H NMR δ 8.42 (s, 1H), 8.40 (d, 2H), 8.01 (d, 2H), 7.51 (m, 4H), 5.55 (br s, 2H), 3.50 (t, 2H), 2.80 (br s, 2H), 2.52 (t, 2H), 2.28 (t, 2H), 1.58 (br s, 13H), 1.20 (m, 4H), 0.88 (br s, 2H); ^{13}C NMR δ 155.91, 131.53, 131.44, 129.42, 128.32, 126.51, 125.22, 124.43, 79.95, 62.86, 49.84, 49.42, 44.86, 41.41, 33.06, 29.35, 29.30, 28.96 (3C), 28.52, 24.70. HRMS (FAB) calcd for $C_{29}H_{41}N_2O_3$ $(M + H)^+$: 465.3112. Found: 465.3118.

Anthracen-9-ylmethyl[5-(5-hydroxypentylamino)pentyl]carbamic acid *tert*-butyl ester (7f): pale-yellow viscous liquid; yield 85%; $R_f = 0.39$, chloroform/methanol/NH_4OH, 90:10:1; ^{1}H NMR δ 8.42 (s, 1H), 8.40 (d, 2H), 8.00 (d, 2H), 7.50 (m, 4H), 5.52 (br s, 2H), 3.60 (t, 2H), 2.80 (br s, 2H), 2.48 (t, 2H), 2.28 (t, 2H), 1.90 (br s, 2H, NH, OH), 1.50 (br s, 11H), 1.45 (m, 4H), 1.22 (m, 2H), 1.19 (m, 2H), 0.92 (m, 2H); ^{13}C NMR δ 155.96, 131.53, 131.44, 129.40, 129.08, 128.31, 126.47, 125.19, 124.41, 79.91, 62.73, 49.97 (2C), 44.86, 41.31, 32.78, 29.92, 29.70, 28.94 (3C), 28.58, 24.83, 23.81. HRMS (FAB) calcd for $C_{30}H_{43}N_2O_3$ $(M + H)^+$: 479.3274. Found: 479.3268.

[3-(Anthracen-9-ylmethyl-*tert*-butoxycarbonylamino)propyl](3-hydroxypropyl)carbamic acid *tert*-butyl ester (8a): pale-yellow viscous liquid; yield 68%; $R_f = 0.38$, hexane/acetone, 3:1; ^{1}H NMR δ 8.42 (s, 1H), 8.39 (d, 2H), 8.00 (d, 2H), 7.50 (m, 4H), 5.50 (br s, 2H), 3.70 (br s, 1H, OH), 3.30 (br s, 2H), 2.85 (br s, 2H), 2.78 (br s, 2H), 2.60 (br s, 2H), 1.60 (br s, 9H), 1.28 (br s, 13H). HRMS (FAB) calcd for $C_{31}H_{43}N_2O_5$ $(M + H)^+$: 523.3172. Found: 523.3183.

[3-(Anthracen-9-ylmethyl-*tert*-butoxycarbonylamino)propyl](4-hydroxybutyl)carbamic acid *tert*-butyl ester (8b): pale-yellow viscous liquid; yield 82%; $R_f = 0.38$, hexane/acetone, 70:30; ^{1}H NMR δ 8.42 (s, 1H), 8.39 (d, 2H), 8.00 (d, 2H), 7.50 (m, 4H), 5.50 (br s, 2H), 3.56 (br s, 2H), 2.84 (br s, 2H), 2.70 (br s, 4H), 2.50 (br s, 1H, OH), 1.60 (br s, 9H), 1.28 (br s, 15H); ^{13}C NMR δ 155.50, 155.44, 131.57, 131.46, 129.47, 128.86, 128.42, 126.66, 125.27, 124.25, 80.15, 79.34, 62.73, 46.06, 44.89, 43.21, 41.70, 29.82, 28.95 (3C, CH_3), 28.68 (3C, CH_3), 28.04, 24.74. HRMS (FAB) calcd for $C_{32}H_{45}N_2O_5$ $(M + H)^+$: 537.3328. Found: 537.3338.

[4-(Anthracen-9-ylmethyl-*tert*-butoxycarbonylamino)butyl](4-hydroxybutyl)carbamic acid *tert*-butyl ester (8d): pale-yellow viscous liquid; yield 71%; $R_f = 0.43$, hexane/acetone, 70:30; ^{1}H NMR δ 8.42 (s, 1H), 8.39 (d, 2H), 8.00 (d, 2H), 7.50 (m, 4H), 5.50 (br s, 2H), 3.62 (t, 2H), 3.00 (br s, 2H), 2.82 (br s, 4H), 2.02 (br s, 1H, OH), 1.60 (br s, 9H), 1.50 (m, 6H), 1.34 (br s, 9H), 1.18 (br s, 2H); ^{13}C NMR δ 155.64, 131.56, 131.49, 129.46, 128.38, 126.54, 125.21, 124.33, 80.08, 79.38, 62.83, 46.99, 46.97, 44.71, 41.48, 29.96, 28.95 (3C, CH_3), 28.78 (3C, CH_3), 26.31, 26.25, 25.22. HRMS (FAB) calcd for $C_{33}H_{46}N_2O_5$ Na $(M + Na)^+$: 573.3299. Found: 573.3325.

[5-(Anthracen-9-ylmethyl-*tert*-butoxycarbonylamino)pentyl](4-hydroxybutyl)carbamic acid *tert*-butyl ester (8e): pale-yellow viscous liquid; yield 69%; $R_f = 0.30$, hexane/acetone, 75:25; ^{1}H NMR δ 8.42 (s, 1H), 8.39 (d, 2H), 8.00 (d, 2H), 7.50 (m, 4H), 5.50 (br s, 2H), 3.62 (br s, 2H), 3.10 (br s, 2H), 2.85 (br s, 4H), 2.40 (br s, 1H, OH), 1.60 (br s, 9H), 1.50 (m, 4H), 1.34 (br s, 9H), 1.18 (br s, 4H), 0.95 (br s, 2H); ^{13}C NMR δ 155.80, 131.54, 131.49, 129.41, 128.32, 126.49, 125.20, 124.39, 79.96, 79.39, 62.72, 47.21, 47.01, 44.82, 41.30, 30.07, 28.95 (3C, CH_3), 28.82 (3C, CH_3), 28.55, 25.27, 24.41 (2C). HRMS (FAB) calcd for $C_{34}H_{48}N_2O_5$ Na $(M + Na)^+$: 587.3455. Found: 587.3480.

[5-(Anthracen-9-ylmethyl-*tert*-butoxycarbonylamino)pentyl](5-hydroxypentyl)carbamic acid *tert*-butyl ester (8f): pale-yellow viscous liquid; yield 61%; $R_f = 0.42$, hexane/acetone, 70:30; ^{1}H NMR δ 8.42 (s, 1H), 8.39 (d, 2H), 8.00 (d, 2H), 7.50 (m, 4H), 5.50 (br s, 2H), 3.62 (br s, 2H), 3.10−2.80 (m, 6H), 1.64 (m, 11H, $3CH_3 + CH_2$), 1.40 (m, 11H, $3CH_3 + CH_2$), 1.25 (m, 6H), 0.90 (br s, 2H); ^{13}C NMR δ 155.71, 131.55, 131.50, 129.41, 128.31, 126.48, 125.21, 124.41, 79.94, 79.38, 63.04, 47.20, 47.00, 44.81, 41.28, 32.71, 28.94 (3C, CH_3), 28.83 (3C, CH_3), 28.54, 28.49, 28.26, 24.43, 23.24. HRMS (FAB) calcd for $C_{35}H_{51}N_2O_5$ $(M + H)^+$: 579.3798. Found: 579.3780.

Toluene-4-sulfonic acid 4-{[3-(anthracen-9-ylmethyl-*tert*-butoxycarbonylamino)propyl]-*tert*-butoxycarbonylamino}butyl ester (9b): pale-yellow viscous liquid; yield 70%; $R_f = 0.35$, hexane/acetone, 75:25; ^{1}H NMR δ 8.42 (s, 1H), 8.39 (d, 2H), 8.00 (d, 2H), 7.78 (d, 2H), 7.48 (m, 4H), 7.28 (d, 2H), 5.50 (br s, 2H), 3.90 (t, 2H), 2.82 (br s, 2H), 2.60 (br s, 4H), 2.40 (s, 3H), 1.58 (br s, 9H, $3CH_3$), 1.42 (br s, 2H), 1.22 (m, 13H, $3CH_3 + 2CH_2$); ^{13}C NMR δ 155.19, 144.87, 133.28, 131.57, 131.43, 130.03, 129.46, 128.42, 128.05, 126.67, 125.29, 124.18, 80.19, 79.38, 70.51, 45.26, 44.71, 43.27, 41.78, 28.95 (3C, CH_3), 28.80, 28.64 (3C, CH_3), 26.46, 24.20, 22.03. HRMS (FAB) calcd for $C_{39}H_{51}N_2O_7S$ $(M + H)^+$: 691.3417. Found: 691.3411.

Toluene-4-sulfonic acid 4-{[4-(anthracen-9-ylmethyl-*tert*-butoxycarbonylamino)butyl]-*tert*-butoxycarbonylamino}butyl ester (9d): pale-yellow viscous liquid; yield 74%; $R_f = 0.43$, hexane/acetone, 75:25; ^{1}H NMR δ 8.42 (s, 1H), 8.39 (d, 2H), 8.00 (d, 2H), 7.78 (d, 2H), 7.48 (m, 4H), 7.28 (d, 2H), 5.50 (br s, 2H), 4.00 (t, 2H), 2.88 (br s, 2H), 2.80−2.62 (m, 4H), 2.40 (s, 3H), 1.58 (br s, 9H, $3CH_3$), 1.38 (m, 13H, $3CH_3 + 2CH_2$), 1.05 (br s, 4H); ^{13}C NMR δ 155.43, 144.89, 133.30, 131.56, 131.49, 130.04, 129.47, 128.39, 128.06, 126.55, 125.23, 124.33, 80.10, 79.42, 70.55, 46.79, 46.20, 44.74, 41.46, 28.95 (3C, CH_3), 28.74 (3C, CH_3), 26.57 (2C), 26.22, 24.51, 22.02.

***N*^{1}-{3-[3-(Anthracen-9-ylmethyl)amino]propylamino}butane-1,4-diamine tetrahydrochloride (11a):** bright-yellow solid; yield 96%; ^{1}H NMR δ 8.72 (s, 1H), 8.28 (d, 2H), 8.16 (d, 2H), 7.64 (t, 2H), 7.58 (t, 2H), 5.20 (br s, 2H), 3.38 (br s, 2H), 3.00 (m, 8H), 2.84 (br s, 2H), 2.12 (br s, 2H), 2.00 (br s, 2H), 1.62 (br s, 4H); ^{13}C NMR δ 130.73, 130.54, 130.17, 129.55, 127.82, 125.59, 122.57, 120.17, 47.38, 44.91 (2C), 44.83, 44.70, 43.19, 39.11, 24.25, 23.09, 22.99 (2C). HRMS (FAB) calcd for $C_{25}H_{37}N_4$ $(M + H - 4HCl)^+$: 393.3013. Found: 393.3020.

***N*-(3-Aminopropyl)-*N*-{3-[(anthracen-9-ylmethyl)amino]propyl}butane-1,4-diamine tetrahydrochloride (11b):** bright-yellow solid; yield 91%; ^{1}H NMR δ 8.73 (s, 1H), 8.28 (d, 2H), 8.17 (d, 2H), 7.64 (t, 2H), 7.58 (t, 2H), 5.18 (s, 2H), 3.30 (t, 2H), 2.96 (m, 10H), 2.10 (m, 2H), 1.90 (m, 2H), 1.60 (br s, 4H); ^{13}C NMR δ 130.70, 130.51, 130.13, 129.51, 127.77, 125.55, 122.54, 120.15, 47.25 (2C), 44.81 (2C), 44.71, 43.12, 36.8, 24.06, 23.05 (2C), 22.97. HRMS (FAB) calcd for $C_{25}H_{37}N_4$ $(M + H - 4HCl)^+$: 393.3013. Found: 393.3018.

***N*-(4-Aminobutyl)-*N*-{3-[(anthracen-9-ylmethyl)amino]propyl}butane-1,4-diamine tetrahydrochloride (11c):** bright-yellow solid; yield 95%; ^{1}H NMR δ 8.80 (s, 1H), 8.40 (d, 2H), 8.19 (d, 2H), 7.66 (t, 2H), 7.60 (t, 2H), 5.21 (s, 2H), 3.40 (t, 2H), 3.02 (t, 2H), 2.92 (m, 6H), 2.82 (t, 2H), 2.11 (m, 2H), 1.62 (m, 8H); ^{13}C NMR δ 130.85, 130.62, 130.29, 129.57, 127.86,

125.64, 122.61, 120.38, 47.26, 47.18, 47.10, 44.86, 44.72, 43.25, 39.06, 24.23, 23.07 (2C), 22.99. HRMS (FAB) calcd for $C_{26}H_{39}N_4$ $(M + H - 4HCl)^+$: 407.3175. Found: 407.3165.

***N*-(4-Aminobutyl)-*N*-{3-[(anthracen-9-ylmethyl)amino]propyl}pentane-1,5-diamine tetrahydrochloride (11d):** bright-yellow solid; yield 88%; ^{1}H NMR δ 8.70 (s, 1H), 8.28 (d, 2H), 8.15 (d, 2H), 7.63 (t, 2H), 7.58 (t, 2H), 5.20 (s, 2H), 3.38 (t, 2H), 3.01 (t, 2H), 2.90 (m, 8H), 2.11 (m, 2H), 1.62 (br s, 8H), 1.28 (m, 2H); ^{13}C NMR δ 130.71, 130.52, 130.14, 129.53, 127.80, 125.57, 122.55, 120.16, 47.70, 47.54, 47.12, 44.84, 44.65, 43.13, 39.10, 25.39 (2C), 24.26, 23.16, 23.08, 22.97. HRMS (FAB) calcd for $C_{27}H_{41}N_4$ $(M + H - 4HCl)^+$: 421.3326. Found: 421.3327.

***N*-[4-(3-Aminopropylamino)butyl]-*N*-anthracen-9-ylmethylbutane-1,4-diamine tetrahydrochloride (11e):** bright-yellow solid; yield 94%; ^{1}H NMR δ 8.79 (s, 1H), 8.40 (d, 2H), 8.19 (d, 2H), 7.68 (t, 2H), 7.60 (t, 2H), 5.21 (s, 2H), 3.28 (t, 2H), 2.92 (m, 10H), 1.92 (m, 2H), 1.80 (m, 2H), 1.70 (br s, 6H); ^{13}C NMR δ 130.69, 130.41, 130.09, 129.49, 127.73, 125.53, 122.52, 120.37, 47.28, 47.20, 47.12, 47.06, 44.81, 42.82, 36.82, 24.05, 23.15, 23.08 (2C), 23.01. HRMS (FAB) calcd for $C_{26}H_{39}N_4$ $(M + H - 4HCl)^+$: 407.3169. Found: 407.3166.

***N*-[4-(4-Aminobutylamino)butyl]-*N*-anthracen-9-ylmethylbutane-1,4-diamine tetrahydrochloride (11f):** bright-yellow solid; yield 86%; ^{1}H NMR δ 8.79 (s, 1H), 8.40 (d, 2H), 8.19 (d, 2H), 7.68 (t, 2H), 7.60 (t, 2H), 5.21 (s, 2H), 3.24 (br s, 2H), 2.92 (br s, 8H), 2.84 (br s, 2H), 1.80 (br s, 2H), 1.64 (br s, 10H); ^{13}C NMR δ 130.75, 130.46, 130.14, 129.53, 127.77, 125.57, 122.57, 120.45, 47.24, 47.20, 47.14 (2C), 47.08, 42.88, 39.09, 24.26, 23.18, 23.12 (2C), 23.10, 23.06. HRMS (FAB) calcd for $C_{27}H_{41}N_4$ $(M + H - 4HCl)^+$: 421.3326. Found: 421.3310.

***N*-[4-(3-Aminopropylamino)butyl]-*N*-anthracen-9-ylmethylpentane-1,5-diamine tetrahydrochloride (11g):** bright-yellow solid; yield 88%; ^{1}H NMR δ 8.79 (s, 1H), 8.40 (d, 2H), 8.19 (d, 2H), 7.66 (t, 2H), 7.60 (t, 2H), 5.20 (s, 2H), 3.22 (t, 2H), 2.90 (m, 10H), 1.92 (m, 2H), 1.66 (m, 8H), 1.40 (m, 2H); ^{13}C NMR δ 130.70, 130.36, 130.07, 129.49, 127.72, 125.54, 122.53, 120.50, 47.64, 47.53, 47.30, 47.05, 44.82, 42.69, 36.84, 25.36, 25.28, 24.07, 23.27, 23.11, 23.09. HRMS (FAB) calcd for $C_{27}H_{41}N_4$ $(M + H- 4HCl)^+$: 421.3326. Found: 421.3319.

***N*-[4-(4-Aminobutylamino)butyl]-*N*-anthracen-9-ylmethylpentane-1,5-diamine tetrahydrochloride (11h):** bright-yellow solid; yield 92%; ^{1}H NMR δ 8.78 (s, 1H,), 8.39 (d, 2H), 8.18 (d, 2H), 7.66 (t, 2H), 7.60 (t, 2H), 5.20 (s, 2H), 3.22 (t, 2H), 2.88 (br s, 8H), 2.80 (m, 2H), 1.74 (m, 2H), 1.62 (br s, 10H), 1.40 (m, 2H); ^{13}C NMR δ 130.70, 130.36, 130.07, 129.49, 127.72, 125.54, 122.53, 120.50, 47.64, 47.53, 47.20, 47.14, 47.06, 42.70, 39.08, 25.36, 25.28, 24.24, 23.27, 23.12 (2C), 23.08. HRMS (FAB) calcd for $C_{28}H_{43}N_4$ $(M + H - 4HCl)^+$: 435.3482. Found: 435.3477.

***N*-[5-(4-Aminobutylamino)pentyl]-*N*-anthracen-9-ylmethylpentane-1,5-diamine tetrahydrochloride (11i):** bright-yellow solid; yield 99%; ^{1}H NMR δ 8.70 (s, 1H), 8.28 (d, 2H), 8.13 (d, 2H), 7.66 (t, 2H), 7.56 (t, 2H), 5.24 (s, 2H), 3.16 (t, 2H), 2.88 (m, 10H), 1.70 (m, 2H), 1.58 (m, 10H), 1.32 (m, 4H); ^{13}C NMR δ 130.69, 130.35, 130.06, 129.49, 127.70, 125.52, 122.52, 120.50, 47.62, 47.56, 47.48, 47.44, 47.11, 42.67, 39.08, 25.42 (2C), 25.34, 25.27, 24.25, 23.27, 23.21, 23.07. HRMS (FAB) calcd for $C_{29}H_{45}N_4$ $(M + H - 4HCl)^+$: 449.3644. Found: 449.3650.

Acknowledgment. This work was supported in part by the Elsa U. Pardee Foundation and the Florida Hospital Gala Endowed Program for Oncologic Research. The authors thank the Chinese Scholarship Council for partial support of C.W. The assistance of Dr. Richard Gardner and Mr. Tito Carias in obtaining the deconvolution microscopy images is also appreciated.

References

(1) Phanstiel, O., IV; Price, H. L.; Wang, L.; Juusola, J.; Kline, M.; Shah, S. M. The Effect of Polyamine Homologation on the Transport and Cytotoxicity Properties of Polyamine−(DNA-Intercalator) Conjugates. *J. Org. Chem*. **2000**, *65*, 5590−5599.

(2) Wang, L.; Price, H. L.; Juusola, J.; Kline, M.; Phanstiel, O., IV. The Influence of Polyamine Architecture on the Transport and Topoisomerase II Inhibitory Properties of Polyamine DNA-Intercalator Conjugates. *J. Med. Chem*. **2001**, *44*, 3682−3691.

(3) Sugiyama, S.; Matsuo, Y.; Maenaka, K.; Vassylyev, D. G.; Matsushima, M.; Kashiwagi, K.; Igarashi, K.; Morikawa, K. The 1.8-A X-ray structure of the *Escherichia coli* PotD protein complexed with spermidine and the mechanism of polyamine binding. *Protein Sci*. **1996**, *5* (10), 1984−1990.

(4) Vassylyev, D. G.; Tomitori, H.; Kashiwagi, K.; Morikawa, K.; Igarashi, K. Crystal structure and mutational analysis of the *Escherichia coli* putrescine receptor. Structural basis for substrate specificity. *J. Biol. Chem*. **1998**, *273* (28), 17604−17609.

(5) Bergeron, R. J.; Feng, Y.; Weimar, W. R.; McManis, J. S.; Dimova, H.; Porter, C.; Raisler, B.; Phanstiel, O. A Comparison of Structure−Activity Relationships between Spermidine and Spermine Analogue Antineoplastics. *J. Med. Chem*. **1997**, *40*, 1475−1494.

(6) Cullis, P. M.; Green, R. E.; Merson-Davies, L.; Travis, N. Probing the mechanism of transport and compartmentalisation of polyamines in mammalian cells. *Chem. Biol*. **1999**, *6* (10), 717−729.

(7) Kramer, D. L.; Miller, J. T.; Bergeron, R. J.; Khomutov, R.; Khomutov, A.; Porter, C. W. Regulation of polyamine transport by polyamines and polyamine analogs. *J. Cell. Physiol*. **1993**, *155*, 399−407.

(8) Kashiwagi, K.; Endo, H.; Kobayashi, H.; Takio, K.; Igarashi, K. Spermidine-preferential uptake systemin *Escherichia coli*. ATP hydrolysis by PotA protein and its association with membrane. *J. Biol. Chem*. **1995**, *270*, 25377−25382.

(9) Kashiwagi, K.; Miyamoto, S.; Nukui, E.; Kobayashi, H.; Igarashi, K. Functions of potA and potD proteins in spermidine-preferential uptake system in *Escherichia coli*. *J. Biol. Chem*. **1993**, *268*, 19358−19363.

(10) Tomitori, H.; Kashiwagi, K.; Sakata, K.; Kakinuma, Y.; Igarashi, K. Identification of a gene for a polyamine transport protein in yeast. *J. Biol. Chem*. **1999**, *274*, 3265−3267.

(11) (a) Bergeron, R. J.; Wiegand, J.; McManis, J. S.; Weimar, W. R.; Smith, R. E.; Algee, S. E.; Fannin, T. L.; Slusher, M. A.; Snyder, P. S. Polyamine Analogue Antidiarrheals: A Structure−Activity Study. *J. Med. Chem*. **2001**, *44*, 232−244. (b) Bergeron, R. J.; Yao, G. W.; Yao, H.; Weimar, W. R.; Sninsky, C. A.; Raisler, B.; Feng, Y.; Wu, Q.; Gao, F. Metabolically Programmed Polyamine Analogue Antidiarrheals. *J. Med. Chem*. **1996**, *39*, 2461−2471. (c) Bergeron, R. J.; Neims, A. H.; McManis, J. S.; Hawthorne, T. R.; Vinson, J. R. T.; Bortell, R.; Ingeno, M. J. Synthetic polyamine analogs as antineoplastics. *J. Med. Chem*. **1988**, *31*, 1183−1190. (d) Casero, R. A., Jr.; Woster, P. M. Terminally Alkylated Polyamine Analogues as Chemotherapeutic Agents. *J. Med. Chem*. **2001**, *44*, 1−26 and references therein.

(12) Delcros, J.-G.; Tomasi, S.; Carrington, S.; Martin, B.; Renault, J.; Blagbrough, I. S.; Uriac, P. Effect of spermine conjugation on the cytotoxicity and cellular transport of acridine. *J. Med. Chem*. **2002**, *45*, 5098−5111.

(13) Wang, C.; Delcros, J.-G.; Biggerstaff, J.; Phanstiel, O., IV. Synthesis and Biological Evaluation of N^1-(Anthracen-9-ylmethyl)triamines as Molecular Recognition Elements for the Polyamine Transporter. *J. Med. Chem*. **2003**, *46*, 2663−2671.

(14) Mandel, J. L.; Flintoff, W. F. Isolation of mutant mammalian cells altered in polyamine transport. *J. Cell. Physiol*. **1978**, *97*, 335−344.

(15) Byers, T. L.; Wechter, R.; Nuttall, M. E.; Pegg, A. E. Expression of a human gene for polyamine transport in Chinese hamster ovary cells. *Biochem. J*. **1989**, *263*, 745−752.

(16) Azzam, T.; Eliyahu, H.; Shapira, L.; Linial, M.; Barenholz, Y.; Domb, A. J. Polysaccharide-Oligoamine Based Conjugates for Gene Delivery. *J. Med. Chem*. **2002**, *45*, 1817−1824.

(17) Stark, P. A.; Thrall, B. D. Meadows, G. G.; Abdul-Monem, M. M. Synthesis and evaluation of novel spermidine derivatives as targeted cancer chemotherapeutic agents. *J. Med. Chem*. **1992**, *35*, 4264−4269.

(18) Cohen, G. M.; Cullis, P.; Hartley, J. A.; Mather, A. Symons, M. C. R.; Wheelhouse, R. T. Targeting of Cytotoxic Agents by Polyamines: Synthesis of a Chloroambucil−Spermidine Conjugate. *J. Chem. Soc., Chem. Commun*. **1992**, 298−300.

(19) Cai, J.; Soloway, A. H. Synthesis of Carboranyl Polyamines for DNA Targeting. *Tetrahedron Lett*. **1996**, *37*, 9283−9286.

(20) Ghaneolhosseini, H.; Tjarks, W.; Sjoberg, S. Synthesis of Novel Boronated Acridines and Spermidines as Possible Agents for BNCT. *Tetrahedron* **1998**, *54*, 3877−3884.

(21) Blagbrough, I. S.; Geall, A. J. Homologation of Polyamines in the Synthesis of Lipo-Spermine Conjugates and Related Lipoplexes. *Tetrahedron Lett*. **1998**, 443−446.

(22) Cullis, P. M.; Merson-Davies, L.; Weaver, R. Mechanism and reactivity of chlorambucil and chlorambucil−spermidine conjugate. *J. Am. Chem. Soc*. **1995**, *117*, 8033−8034.

(23) Aziz, S. M.; Yatin, M.; Worthen, D. R.; Lipke, D. W.; Crooks, P. A. A novel technique for visualising the intracellular localization and distribution of transported polyamines in cultured pulmonary artery smooth muscle cells. *J. Pharm. Biomed. Anal.* **1998**, *17*, 307−320.
(24) Blagbrough, I. S.; Geall, A. J. Practical Synthesis of Unsymmetrical Polyamine Amides. *Tetrahedron Lett.* **1998**, 439−442.
(25) Saab, N. H.; West, E. E.; Bieszk, N. C.; Preuss, C. V.; Mank, A. R.; Casero, R. A.; Woster, P. M. Synthesis and Evaluation of Polyamine Analogues as Inhibitors of Spermidine/Spermine−N^1-Acetyltransferase (SSAT) and as Potential Antitumor Agents. *J. Med. Chem.* **1993**, *36*, 2998−3004.
(26) Kumar, C. V.; Asuncion, E. H. DNA Binding Studies and Site Selective Fluorescence Sensitization of an Anthryl Probe. *J. Am. Chem. Soc.* **1993**, *115*, 8547−8553.
(27) Rodger, A.; Taylor, S.; Adlam, G.; Blagbrough, I. S.; Haworth, I. S. Multiple DNA Binding Modes of Anthracene-9-carbonyl-N^1-spermine. *Bioorg. Med. Chem.* **1995**, *3* (6), 861−872.
(28) Wang, C.; Abboud, K. A.; Phanstiel, O., IV Synthesis and Characterization of N^1-(4-toluenesulfonyl)-N1-(9-anthracenemethyl)triamines. *J. Org. Chem.* **2002**, *67*, 7865−7868.
(29) Porter, C. W.; Cavanaugh, P. F.; Ganis, B.; Kelly, E.; Bergeron, R. J. Biological properties of N-4 and N-1,N-8-spermidine derivatives in cultured L1210 leukemia cells. *Cancer Res.* **1985**, *45*, 2050−2057.
(30) Porter, C. W.; Ganis, B.; Vinson, T.; Marton, L. J.; Kramer, D. L.; Bergeron, R. J. Comparison and characterization of growth inhibition in L1210 cells by alpha-difluoromethylornithine, an inhibitor of ornithine decarboxylase, and N1,N8-bis(ethyl)-spermidine, an apparent regulator of the enzyme. *Cancer Res.* **1986**, *46*, 6279−6285.
(31) Bergeron, R. J.; McManis, J. S.; Liu, C. Z.; Feng, Y.; Weimar, W. R.; Luchetta, G. R.; Wu, Q.; Ortiz-Ocasio, J.; Vinson, J. R. T.; Kramer, D.; Porter, C. Antiproliferative Properties of Polyamine Analogues: A Structure−Activity Study. *J. Med. Chem.* **1994**, *37*, 3464−3476.
(32) Belting, M.; Persson, S.; Fransson, L.-A. Proteoglycan involvement in polyamine uptake. *Biochem. J.* **1999**, *338*, 317−323.
(33) (a) Schindler, M.; Koppel, D. E.; Sheetz, M. P. Modulation of membrane protein lateral mobility by polyphosphates and polyamines. *Proc. Natl. Acad. Sci. U.S.A.* **1980**, *77* (3), 1457−1461. (b) Ballas, S. K.; Mohandas, N.; Marton, L. J.; Shohet, S. B. Stabilization of erythrocyte mebranes by polyamines. *Proc. Natl. Acad. Sci. U.S.A.* **1983**, *80* (7), 1942−1946. (c) Schuber, F. Influence of polyamines on membrane functions. *Biochem. J.* **1989**, *269*, 1−10.
(34) Soulet, D.; Covassin, L.; Kaouass, M.; Charest-Gaudreault, R.; Audette, M.; Poulin, R. Role of endocytosis in the internalisation of spermidine−C2-BODIPY, a highly fluorescent probe of polyamine transport. *Biochem. J.* **2002**, *367*, 347−357.
(35) Fransson, L.-A. Glypicans. *Int. J. Biochem. Cell Biol.* **2002**, *1348*, 1−5.
(36) Belting, M.; Borsig, L.; Fuster, M. M.; Brown, J. R.; Persson, L.; Fransson, L.-A.; Esko, J. D. Tumor attenuation by combined heparan sulfate and polyamine depletion. *Proc. Natl. Acad. Sci. U.S.A.* **2002**, *99*, 371−376.
(37) Mislick, K. A.; Baldeschwieler, J. D. Evidence for the role of proteoglycans in cation-mediated gene transfer. *Proc. Natl. Acad. Sci. U.S.A.* **1996**, *93*, 12349−12354.
(38) Mounkes, L. C.; Zhong, W.; Cipres-Palacin, G.; Heath, T. D.; Debs, R. J. Proteoglycans Mediate Cationic Liposome−DNA Complex-Based Gene Delivery in Vitro and in Vivo. *J. Biol. Chem.* **1998**, *273*, 26164−26170.
(39) Bergeron, R. J.; McManis, J. S.; Weimar, W. R.; Schreier, K. M.; Gao, F.; Wu, Q.; Ortiz-Ocasio, J.; Luchetta, G. R.; Porter, C.; Vinson, J. R. T. The role of charge in polyamine analog recognition. *J. Med. Chem.* **1995**, *38*, 2278−2285.
(40) Porter, C.; Miller, J.; Bergeron, R. J. Aliphatic chain-length specificity of the polyamine transport system in ascites L1210 leukemia cells. *Cancer Res.* **1984**, *44*, 126−128.
(41) Xia, C. Q.; Yang, J. J.; Ren, S.; Lien, E. J. QSAR analysis of polyamine transport inhibitors in L1210 cells. *J. Drug Targeting* **1998**, *6* (1), 65−77.
(42) O'Sullivan, M. C.; Golding, B. T.; Smith, L. L.; Wyatt, I. Molecular features necessary for the uptake of diamines and related compounds by the polyamine receptor of rat lung slices. *Biochem. Pharmacol.* **1991**, *41*, 1839−1848.
(43) Kuksa, V.; Buchan, R.; Lin, P. K. T. Synthesis of Polyamines, Their Derivatives, Analogues and Conjugates. *Synthesis* **2000**, No. 9, 1189−1207.
(44) Alhonen-Hongisto, L.; Seppanen, P.; Janne, J. Intracellular putrescine and spermidine deprivation induces increased uptake of the natural polyamines and methylglyoxal bis(guanylhydrazone). *Biochem. J.* **1980**, *192*, 941−945.
(45) Minchin, R. F.; Raso, A.; Martin, R. L.; Ilett, K. F. Evidence for the existence of distinct transporters for the polyamines putrescine and spermidien in B16 melanoma cells. *Eur. J. Biochem.* **1991**, *200*, 457−462.
(46) Rinehart, C. A. J.; Chen, K. Y. Characterization of the polyamine transport system in mouse neuroblastoma cells. Effects of sodium and system A amino acids. *J. Biol. Chem.* **1984**, *259*, 4750−4756.
(47) Mosmann, T. Rapid colorimetric assay for cellular growth and survival: application to proliferation and cytotoxicity assays. *J. Immunol. Methods* **1983**, *65*, 55−63.
(48) Clément, S.; Delcros, J. G.; Feuerstein, B. G. Spermine uptake is necessary to induce haemoglobin synthesis in murine erythroleukemia cells. *Biochem. J.* **1995**, *312*, 933−938.
(49) Cheng, Y.-C.; Prusoff, W. H. Relationship between the inhibition constant (Ki) and the concentration of inhibitor which causes 50% inhibition (IC50) of an enzymatic reaction. *Biochem. Pharmacol.* **1973**, *22*, 3099−3108.
(50) Torossian, K.; Audette, M.; Poulin, R. Substrate protection against inactivation of the mammalian polyamine transport system by 1-ethyl-3-(3-dimethylaminopropyl)-carbodiimide. *Biochem. J.* **1996**, *319*, 21−26.
(51) Covassin, L.; Desjardins, M.; Charest-Gaudreault, R.; Audette, M.; Bonneau, M. J.; Poulin, R. Synthesis of spermidine and norspermidine dimers as high affinity polyamine transport inhibitors. *Bioorg. Med. Chem. Lett.* **1999**, *9*, 1709−1714.
(52) Bergeron, R. J.; Müller, R.; Bussenius, J.; McManis, J. S.; Merriman, R. L.; Smith, R. E.; Yao, H.; Weimar, W. R. Synthesis and Evaluation of Hydroxylated Polyamine Analogues as Antiproliferatives. *J. Med. Chem.* **2000**, *43*, 224−235.

JM020598G